

Mechanical and Physical Properties of Carbon Fiber Reinforced Aluminium Matrix Composites Fabricated by Powder Metallurgy Technique

Mostafa Eid Abd EL-Maboud^{1*}, Saleh Mohammed Kayetbay¹, and Ahmed Mohamed El-Assal¹

¹Benha Faculty of Engineering, Benha, Egypt

ABSTRACT : Carbon fiber reinforced aluminium composites are significantly used in lightweight applications. Powder metallurgy is considered one of the most commonly used methods in manufacturing metal matrix composites due to its low cost and high versatility. The effect of carbon fiber weight fractions and sintering temperatures on the sintered density and microhardness of composites were studied. The percentages of weight fraction of reinforcement were (10wt. %, 20wt. %, and 30wt. %) while the sintering temperatures were (530 °C, 560 °C and 590 °C). The microstructure of composites indicated that CF distributed uniformly in the Al matrix, while EDX results confirmed the absence of harmful intermediate phases. Regression analysis was used to estimate the studied properties of composites with six samples for validation. Results showed that the density and hardness of composites decreased with an increase in carbon fiber percentage. According to the analysis of variance (ANOVA), the sintering temperature had a higher influence than the weight fraction of reinforcement in analyzed properties.

KEYWORDS Carbon fiber, Powder metallurgy, Metal matrix composites, Analysis of variance.

Date of Submission: 29-12-2020

Date of acceptance: 10-01-2021

I. INTRODUCTION

The global need for low cost, rigid and lightweight materials has changed the research into composites materials to satisfy all engineering sectors demands. Metal matrix composites, in particular, have increased its use in industrial applications due to their superb performance [1,2]. Aluminium composites have attractive mechanical and physical properties such as high stiffness, strength, low density and other excellent properties, making them optimal for automotive, aviation, and structural materials [3–7].

Ceramic materials such as SiC, B₄C, alumina and carbon materials are used as reinforcements in aluminium matrix composites. Carbon has many allotropes in nature, including graphite, carbon nanotubes, graphene, diamond and carbon fiber (CF) with superior mechanical, thermal and electrical properties which are desirable materials for reinforcing aluminium [8]. CF is a fascinating, available and low-cost carbonaceous material with unusual mechanical properties [9]. Carbon fiber reinforced aluminium composites (CF/Al) are widely in aerospace applications such as its use in the waveguide antenna mast of Hubble Space Telescope [10].

Processing CF/Al composites are classified into two main categories: first is a liquid state and second is solid state. Several researchers have produced CF/Al composites through liquid state processes such as stir casting, squeeze casting and liquid infiltration [8–15]. However, the low cost and simplicity of manufacturing composites by these methods, the interfacial interactions due to high temperatures, wettability problem, and non-uniformity distribution of reinforcements in the matrix, restrict its use in a wide range. Surface modification such as electroless coating and adding alloying elements to the matrix has been used to solve the mentioned problems [16-18]. Powder metallurgy is a solid-state manufacturing technique which occurs at relatively low temperatures. Thus, the process helps to minimize the interfacial reactions between the matrix and reinforcement and the interfacial phase (Al₄C₃) which deteriorates the properties of composites [22,23].

Several studies focused on the effect of CF on the properties of CF/Al composites [24–28]. Investigation processing parameters especially compacting pressure, sintering temperature, and percentage of reinforcement together has yet to be studied. This was the motivation behind this study. The present

investigation covers these parameters for CF/Al composites and their effects on mechanical and physical properties.

II. EXPERIMENTAL PROCEDURES

2.1 Materials

The matrix is Al powders with an average diameter of 60 microns which possesses irregular potato shape, as shown in fig.1 a and are supplied by (Research-Lab Chem Industries, India). The milled CF in fig.1 b has a diameter of 7 microns and a length of 100 microns purchased from Easy Composite Ltd, England.

2.2 Fabrication of Composites

Samples were produced by mixing certain levels of CF with Al powders. Mixed powders were then uniaxially cold-pressed in a 12 mm high-speed steel die at 100 KN for 2 min by a universal test machine (WAW-600D) at room temperature. Paraffin wax was used as a die lubricant. After the compacting process, samples were sintered at certain levels of temperature for 30 min in a muffle furnace. During the sintering process, the heating rate was 12°C/min, while the cooling rate was 10°C/min to minimize the thermal shocks on samples. Schematic illustration of the preparation of Cf/Al composites is shown in fig.2.

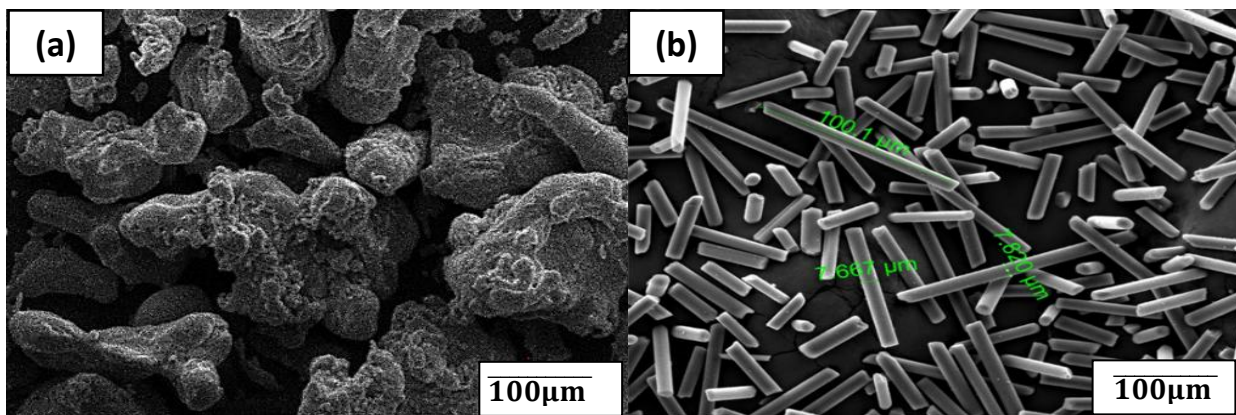


Fig.1. SEM micrographs of powders; (a) Al, and (b) CF.

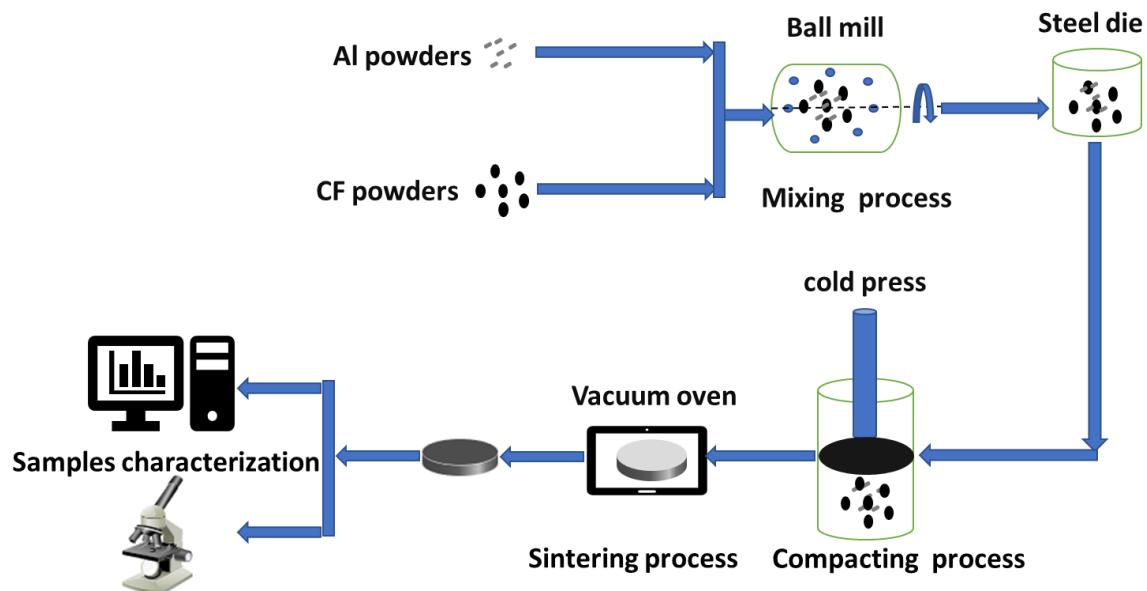


Fig.2. Schematic representation of the steps for preparing Cf/Al composites.

2.3 Characterization of Composites

Quanta 250 field emission scanning electron microscope (FE-SEM) is used to show the microstructure of powders and sintered composites. The phase composition of composites was analyzed using X-ray diffraction (XRD) (model x, pert PRO PANalytical) with Cu α radiation ($\lambda = 0.15406$ nm). The green and sintered densities of composites were measured using the Automatic Density Analyzer (ULTRAPYC 1200e) with three

average readings. The Vickers microhardness test was applied to sintered samples by microhardness tester according to the ASTM E92 with five readings as the average, which were randomly selected at different positions on the samples.

III. RESULTS AND DISCUSSION

3.1 Microstructure of Composites

The EDAX analysis of Al powders in fig.3 shows a high peak of Al with a small percentage of oxygen content. Fig.4 shows SEM images of CF/Al composites consolidated at 560°C which the Al matrix is in grey, while the black is CF. Reinforcement particles are homogeneously distributed in the matrix in the plane normal to the direction of compaction. Most of CF particles are broken during milling operations and maintain their initial shapes. Porosity appears in composites, especially at the interface with some agglomerations at 30 wt.%CF/Al composites. Fig.5 displays the XRD pattern of CF/Al composites consolidated at 590°C. The patterns reveal that the presence of Al peaks as the main element at $2\theta=38.4, 44.60, 64.95, 78.09, 82.30^\circ$ correspond to (111), (200), (220), (311), and (222) crystal planes and a low-intensity peak at $2\theta=26.2^\circ$ corresponds to (002) for CF at a higher percentage of reinforcement. Al_4C_3 isn't detected in all composites, indicating that no chemical reactions have occurred between reinforcement and matrix.

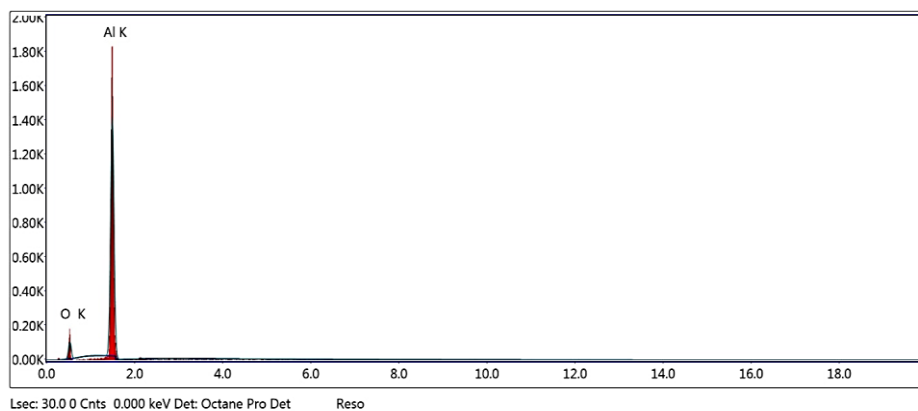


Fig.3.The EDAX of received Al powders.

3.2 Green and Sintered Density

Fig.6 shows the effect of compacting pressure on composites relative density. The relative density of composites increases with an increase of compacting pressure up to 100 KN. After this value, it tends to remain constant, so the compacting process was carried out at 100 KN. When pressure is applied, the particles begin to rearrange to fill spaces between them, leading to a reduction in the porosity of composites. Table 1 presents the observed results of green, sintered density, and microhardness of composites. The main effects plot in fig.7 reveals that as reinforcement percentage increases, the green density reduces. This reduction in density can be attributed to the lower density of CF (1.8g/cc) than Al (2.7g/cc). The addition of hard ceramics powders can restrict the densification rate and increase the needed pressure for the compaction process. Moreover, an increase in CF content increases agglomerations and gaps in the structure (see fig.4), which reduces the density of composites. Individual plots in fig. 8 (a) and (b) describe the influence of reinforcement percentage and sintering temperature on the sintered density of composites. The sintered density decreases with the incorporation of CF, and this supports the previous interpretation and was consistent with the previous studies [29,30]. On the other hand, the sintered density of composites increases until 560°C then it decreases.

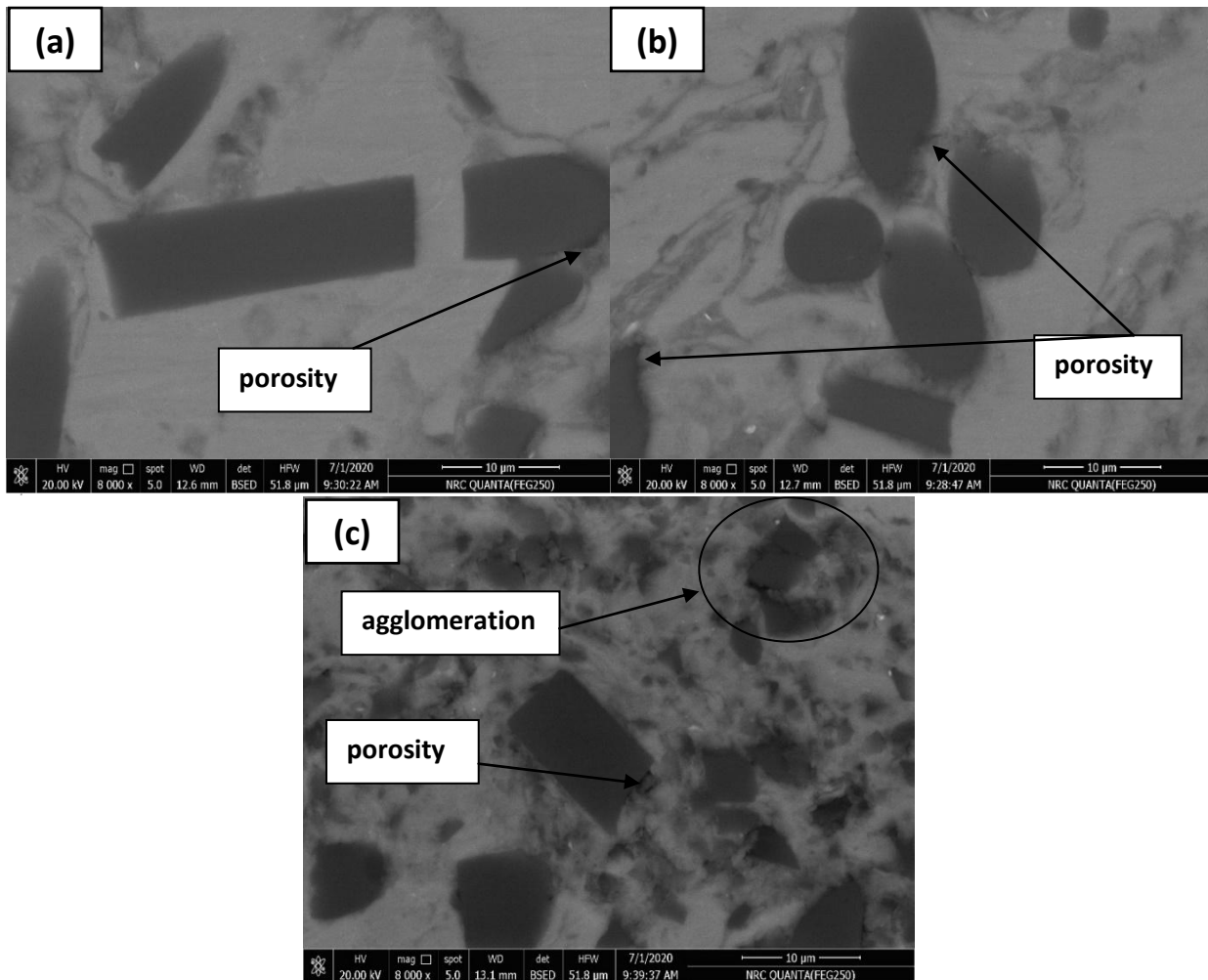


Fig.4. SEM images for composites consolidated at 560 °C; (a) 10wt.% (b) 20wt.%, and (c) 30wt.%.

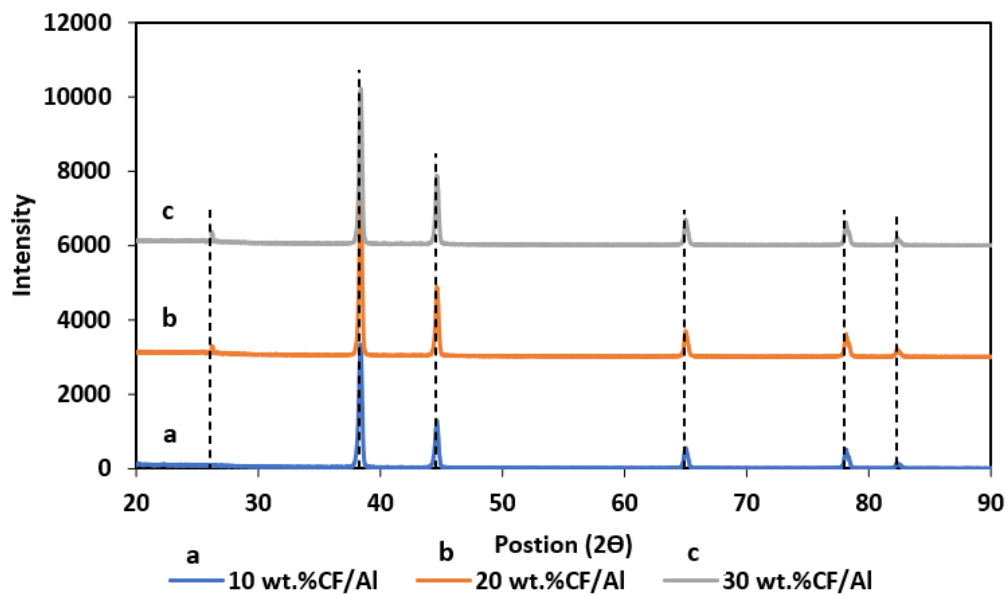


Fig.5. XRD results for composites consolidated at 590 °C ; (a) 10wt.% (b) 20wt.%, and (c) 30wt.%.

The higher diffusion of atoms was induced at a higher sintering temperature, resulting in higher densification [31]. Equation.1 supports the previous observation [32].

$$D = D_0 \exp\left(\frac{-Q}{RT}\right) \tag{1}$$

Where D is the diffusion coefficient, D₀ is constant, Q is the activation energy, R is Boltzman’s constant and T is the temperature.

However, beyond 560°C, the density begins to decrease due to an excess of heat absorption, which leads to volumetric expansion and swelling of the composites [33]. The regression analysis in Equation.2 shows the correlation between sintered density and studied variables. This equation is validated by six samples of experimental results within an error of 6.45 %.

$$Ds=2.982 - 0.00498 Pr - 0.00109 Ts. \tag{2}$$

Where Ds is sintered density g/cc, Pr is reinforcement percentage by weight in gram and Ts is the sintered temperature in Celsius.

3.3 Microhardness

Individual plots in fig. 9 (a) and (b) show the microhardness versus weight percentage of CF and sintered temperature. The microhardness of composites is shown to be decreased as both reinforcement weight fractions, and sintered temperatures increase. The high amount of reinforcement increases the agglomerations and pores content, which reduces the bonding between reinforcement and matrix and the hardness values. While at the elevated temperatures, fast diffusion of CF in the Al matrix which reinforcement is not fully wetted to the matrix. At higher sintering temperatures, the atoms vibrated with higher energy and have the ability to break bonds and consequently, the resistance of composites to penetration is reduced [34]. Equation.3 obtained from the regression analysis is shown below:

$$MH = 181 - 0.5000 Pr - 0.2000 Ts. \tag{3}$$

Where MH is Vickers microhardness, Pr is reinforcement percentage by weight in gram and Ts is the sintered temperature in Celsius.

Table 1. Experimental observations.

Samples	Reinforcement Percentage (%)	Sintering Temperature (°C)	Green Density (g/cc)	Sintered Density (g/cc)	Microhardness (HV)
1	10	530	2.111	2.332	70
2	10	560	2.194	2.453	64
3	10	590	2.146	2.212	59
4	20	560	2.105	2.339	57
5	20	590	2.076	2.195	51
6	20	530	1.976	2.245	64
7	30	590	1.898	2.210	50
8	30	530	1.971	2.236	62
9	30	560	1.867	2.251	51

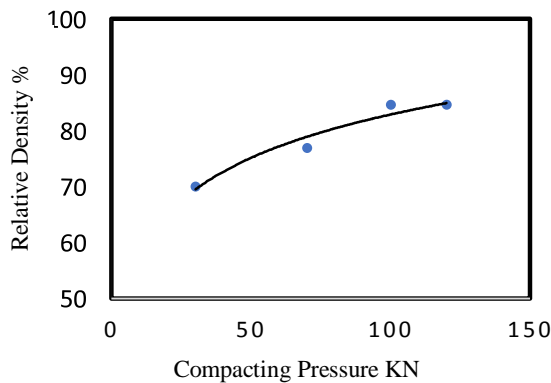


Fig.6. Effect of compacting pressure on relative density of green composites.

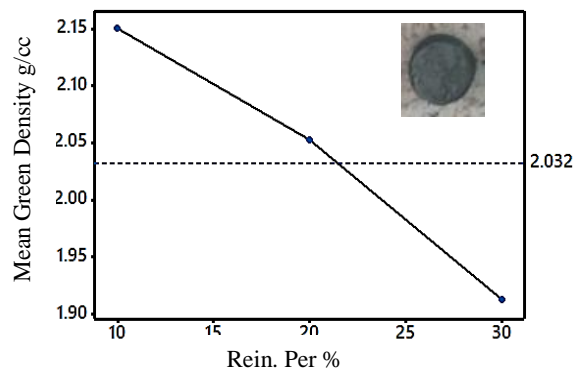


Fig.7. Main effects plot of green density with reinforcement percentage.

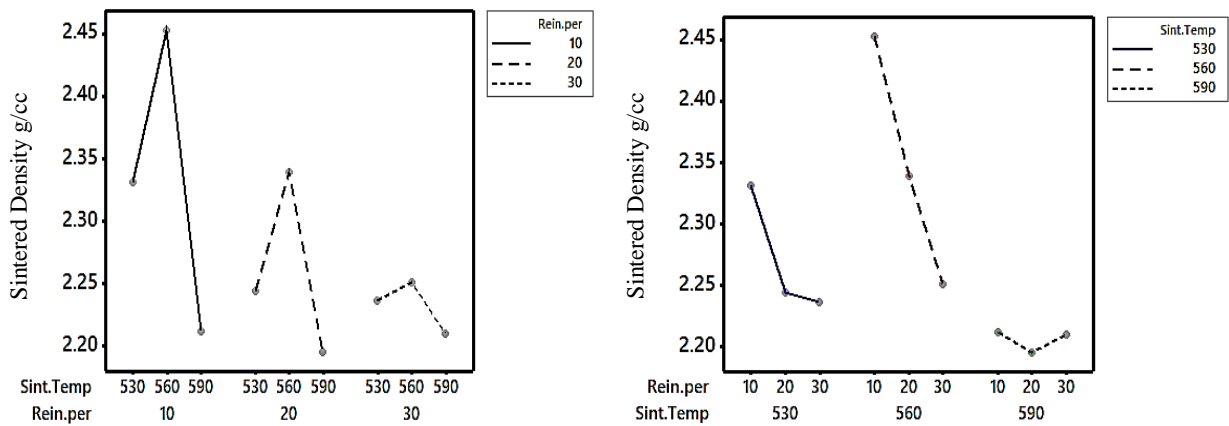


Fig.8. Individual plot for sintered density with respect to; (a) Reinforcement percentage, (b) Sintering temperature.

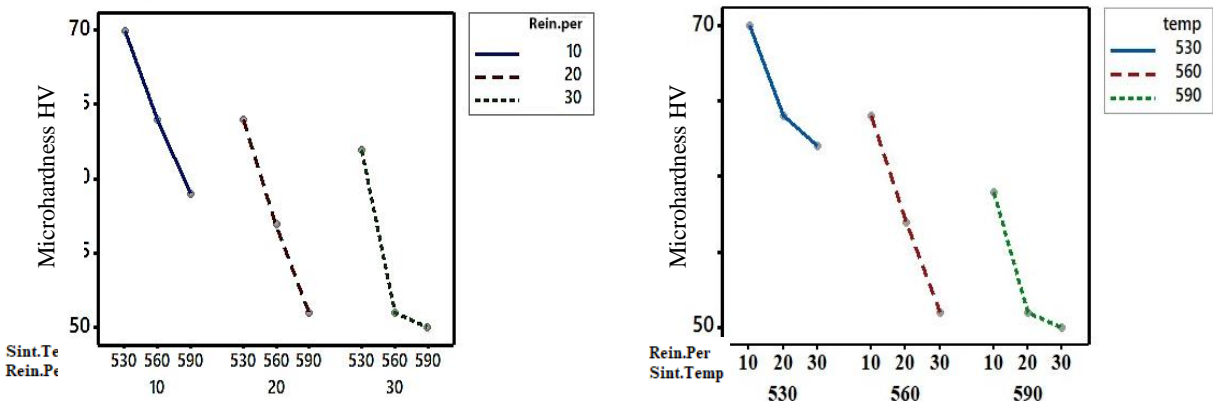


Fig.9. Individual plot for microhardness with respect to; (a) Reinforcement percentage, (b) Sintering temperature.

3.4 Analysis of Variance

Analysis of variance (ANOVA) is used to show the extent to which variables influence studied response. Table 2. shows the results of (ANOVA) on sintered density. For statistics, reinforcement percentage and sintered temperature haven't significantly affected on the sintered density because their P-Value for both is larger than 5 %. It is found that sintered temperature has a more significant influence than reinforcement percentage. The contribution percentage of sintering temperature is 53.67%, while the reinforcement percentage is contributed only to 28%. For the microhardness analysis, the trend was the same. The contribution percentage of sintering temperature is 57.14%, and the reinforcement percentage is 40.56%. Because their p-value is smaller than 5 %, so they obviously contributed to microhardness results, as shown in table 3.

Table 2. Results of the ANOVA for sintered density

Source	DF	Adj S.S.	Adj MS	F-Value	P-Value
Rein. Per	2	0.01592	0.007959	3.11	0.153
Sintered temp	2	0.03030	0.015151	5.93	0.064
Error	4	0.01023	0.002557		
Total	8	0.05645			

Table 3. Results of the ANOVA for microhardness

Source	DF	Adj S.S.	Adj MS	F-Value	P-Value
Rein. Per	2	158.00	79	31.6	0.153
Sintered temp	2	224	112	44.8	0.002
Error	4	10	2.500		
Total	8	392			

IV. CONCLUSION

CF/Al composites were successfully produced by a powder metallurgy technique. The SEM images show that the fibers are distributed in the matrix homogeneously. The optimum compaction pressure for composites was 100 KN. The sintered density decreased with an increase in CF percentage while increased with increasing sintering temperature and achieved the maximum value at temperature 560 °C, then the value was reduced. Both CF percentage and sintered temperature affect negatively on microhardness values. The sintered temperature has more effect than the reinforcement percentage in the studied properties.

REFERENCES

- [1]. M. Kok, Production and mechanical properties of Al₂O₃ particle-reinforced 2024 aluminium alloy composites, *J. Mater. Process. Technol.* 161 (2005) 381–387.
- [2]. D.K. Sharma, D. Mahant, G. Upadhyay, Manufacturing of metal matrix composites: A state of review, *Mater. Today Proc.* (2020).
- [3]. P. Garg, A. Jamwal, D. Kumar, K.K. Sadasivuni, C.M. Hussain, P. Gupta, Advance research progresses in aluminium matrix composites: manufacturing & applications, *J. Mater. Res. Technol.* (2019).
- [4]. S. Arivukkarasan, V. Dhanalakshmi, B. Stalin, M. Ravichandran, Mechanical and tribological behaviour of tungsten carbide reinforced aluminum LM4 matrix composites, *Part. Sci. Technol.* 36 (2018) 967–973.
- [5]. N. Idusuyi, J.I. Olayinka, Dry sliding wear characteristics of aluminium metal matrix composites: a brief overview, *J. Mater. Res. Technol.* (2019).
- [6]. D.K. Koli, G. Agnihotri, R. Purohit, Advanced aluminium matrix composites: The critical need of automotive and aerospace engineering fields, *Mater. Today Proc.* 2 (2015) 3032–3041.
- [7]. A.K. Singh, S. Soni, R.S. Rana, A Critical Review on Synthesis of Aluminum Metallic Composites through Stir Casting: Challenges and Opportunities, *Adv. Eng. Mater.* (2020) 2000322.
- [8]. Y. Huang, Q. Ouyang, D. Zhang, J. Zhu, R. Li, H. Yu, Carbon materials reinforced aluminum composites: a review, *Acta Metall. Sin. (English Lett.)* 27 (2014) 775–786.
- [9]. K. Shirvanimoghaddam, S.U. Hamim, M.K. Akbari, S.M. Fakhrhoseini, H. Khayyam, A.H. Pakseresht, E. Ghasali, M. Zabet, K.S. Munir, S. Jia, Carbon fiber reinforced metal matrix composites: Fabrication processes and properties, *Compos. Part A Appl. Sci. Manuf.* 92 (2017) 70–96.
- [10]. D.B. Miracle, Metal matrix composites—from science to technological significance, *Compos. Sci. Technol.* 65 (2005) 2526–2540.
- [11]. G. Kaptay, T. Bérczy, On the asymmetrical dependence of the threshold pressure of infiltration on the wettability of the porous solid by the infiltrating liquid, *J. Mater. Sci.* 40 (2005) 2531–2535.
- [12]. H. Naji, S.M. Zebarjad, S.A. Sajjadi, The effects of volume percent and aspect ratio of carbon fiber on fracture toughness of reinforced aluminum matrix composites, *Mater. Sci. Eng. A* 486 (2008) 413–420.
- [13]. B.B. Singh, M. Balasubramanian, Processing and properties of copper-coated carbon fibre reinforced aluminium alloy composites, *J. Mater. Process. Technol.* 209 (2009) 2104–2110.
- [14]. T. Shalu, E. Abhilash, M.A. Joseph, Development and characterization of liquid carbon fibre reinforced aluminium matrix composite, *J. Mater. Process. Technol.* 209 (2009) 4809–4813.
- [15]. H.A. Alhashmy, M. Nganbe, Laminate squeeze casting of carbon fiber reinforced aluminum matrix composites, *Mater. Des.* 67 (2015) 154–158.
- [16]. J. Zhang, S. Liu, Y. Lu, Y. Dong, T. Li, Fabrication process and bending properties of carbon fibers reinforced Al-alloy matrix composites, *J. Mater. Process. Technol.* 231 (2016) 366–373.
- [17]. A. Alten, E. Erzi, Ö. Gürsoy, G.H. Ağaoğlu, D. Dispinar, G. Orhan, Production and mechanical characterization of Ni-coated carbon fibers reinforced Al-6063 alloy matrix composites, *J. Alloys Compd.* 787 (2019) 543–550.
- [18]. M. Baghi, B. Niroumand, R. Emadi, Fabrication and characterization of squeeze cast A413-CSF composites, *J. Alloys Compd.* 710 (2017) 29–36.
- [19]. Y. Tang, L. Liu, W. Li, B. Shen, W. Hu, Interface characteristics and mechanical properties of short carbon fibers/Al composites with different coatings, *Appl. Surf. Sci.* 255 (2009) 4393–4400.
- [20]. J.C. Shi, Y.H. Li, G.C. Yao, P.F. Yan, H. Liu, Effect of Mg on Microstructure and Mechanical Properties of Copper-Coated Short Carbon Fiber Reinforced Al Alloy Matrix Composite, in: *Adv. Mater. Res., Trans Tech Publ*, 2012: pp. 348–353.
- [21]. Y. Xue, W. Chen, Q. Zhao, Y. Fu, Electroless carbon fibers: A new route for improving mechanical property and wettability of composites, *Surf. Coatings Technol.* 358 (2019) 409–415.
- [22]. K. Kallip, N.K. Babu, K.A. AlOgab, L. Kollo, X. Maeder, Y. Arroyo, M. Leparoux, Microstructure and mechanical properties of near net shaped aluminium/alumina nanocomposites fabricated by powder metallurgy, *J. Alloys Compd.* 714 (2017) 133–143.
- [23]. J.M. d Torralba, C.E. Da Costa, F. Velasco, P/M aluminum matrix composites: an overview, *J. Mater. Process. Technol.* 133 (2003) 203–206.
- [24]. J.-F. Silvain, A. Veillère, Y. Lu, Copper-carbon and aluminum-carbon composites fabricated by powder metallurgy processes, in: *J. Phys. Conf. Ser.*, IOP Publishing, 2014: p. 12015.
- [25]. H. Kurita, E. Feuillet, T. Guillemet, J.-M. Heintz, A. Kawasaki, J.-F. Silvain, Simple fabrication and characterization of discontinuous carbon fiber reinforced aluminum matrix composite for lightweight heat sink applications, *Acta Metall. Sin. (English Lett.)* 27 (2014) 714–722.

- [26]. M. Deshpande, M.R. Gondil, R. Waikar, T.S. Mahata, Processing of Carbon fiber reinforced Aluminium (7075) metal matrix composite, in: Int. Conf. Renew. Energy Mater. Sustain., 2016.
- [27]. H. Junaedi, H.S. Abdo, K.A. Khalil, A.A. Almajid, Aluminum-Carbon Metal Matrix Composites: Effect of Carbon Fiber and Aspect Ratio on the Mechanical Properties, in: Adv. Mater. Res., Trans Tech Publ, 2015: pp. 119–122.
- [28]. B.T.S. AL-Mosawi, D. Wexler, A. Calka, Characterization and Properties of Aluminium Reinforced Milled Carbon Fibres Composites Synthesized by Uniball Milling and Uniaxial Hot Pressing, Met. Mater. Int. (2020) 1–24.
- [29]. M. Deshpande, R. Gondil, R. Waikar, S.V.S.N. Murty, T.S. Mahata, Processing and Characterization of Carbon Fiber Reinforced Aluminium7075, Mater. Today Proc. 5 (2018) 7115–7122.
- [30]. M. Rashad, F. Pan, Z. Yu, M. Asif, H. Lin, R. Pan, Investigation on microstructural, mechanical and electrochemical properties of aluminum composites reinforced with graphene nanoplatelets, Prog. Nat. Sci. Mater. Int. 25 (2015) 460–470.
- [31]. K.H. Min, S.P. Kang, D.-G. Kim, Y. Do Kim, Sintering characteristic of Al₂O₃-reinforced 2xxx series Al composite powders, J. Alloys Compd. 400 (2005) 150–153.
- [32]. W.D. Callister, D.G. Rethwisch, Materials science and engineering: an introduction, John wiley & sons New York, 2007.
- [33]. M.M. Rahman, R.M. Shahmi, H.Y. Rahman, Effect of Sintering Temperature and Holding Time to the Final Characteristics of Fecral Powder Compacts Formed at Elevated Temperature Through Die Compaction Method, in: J. Phys. Conf. Ser., IOP Publishing, 2018: p. 12030.
- [34]. D.S. Sri Endah Susilowati, Effect of Sintering Temperature on the Mechanical Properties for a Cu-Sn-Zn-C Alloy Produced by Powder Metallurgy, Int. J. Metall. Eng. (2017).

Mostafa Eid Abd EL-Maboud, et. al. "Mechanical and Physical Properties of Carbon Fiber Reinforced Aluminium Matrix Composites Fabricated by Powder Metallurgy Technique." *American Journal of Engineering Research (AJER)*, vol. 10(1), 2021, pp. 134-141.